

**DEVELOPMENT OF AUTONOMOUS DRONE FOR
MULTIPURPOSE FUNCTIONS**

SIM KAI SHENG

UNIVERSITI SAINS MALAYSIA

2018

**DEVELOPMENT OF AUTONOMOUS DRONE FOR
MULTIPURPOSE FUNCTIONS**

by

SIM KAI SHENG

**Thesis submitted in partial fulfilment of the
requirements for the degree of
Bachelor of Engineering (Electrical Engineering)**

JUNE 2018

ACKNOWLEDGEMENT

I would like to express gratitude toward my supervisor, Dr. Teh Jiashen for his grant sponsorship, and more importantly, his guidance, sharing of thoughts and knowledge throughout the project implementation. I would also wish to thank my FYP examiner, Dr. Khairunaz bin Mat Desa for providing invaluable comments and suggestions as well as evaluations.

Special thanks to the final year project coordinators, Associate Professor Dr. Bakhtiar Affendi bin Rosdi, Associate Professor Ir. Dr. Mohamad Kamarol bin Mohd Jamil and Associate Professor Dr. Rosmiwati bt. Mohd Mokhtar for the effort on arranging and conducting seminars for final year students so that the project preparation runs smoothly.

Besides that, I also want to thank my family and friends who motivated me in many ways. I would like to also underline gratitude and appreciation to my mother, Lee Choon Lay, who have raised me up and provided endless supports and love for me. I also wish to thank my friends, Yew Chang Chern, who shared his knowledge about drones, and my Innovate Malaysia competition teammates, Ooi Yoong Khang and Cheong Leong Kean for their ideas and motivations.

Lastly, I would like to thank the School of Electrical and Electronic Engineering, Universiti Sains Malaysia for everything they have imparted me with, toward being a wellversed and knowledgeable engineer.

TABLE OF CONTENTS

ACKNOWLEDGEMENT	i
TABLE OF CONTENTS	ii
LIST OF TABLES	iv
LIST OF FIGURES	v
LIST OF ABBREVIATIONS	x
ABSTRAK	xiv
ABSTRACT	xv
CHAPTER 1 INTRODUCTION	1
1.1 Background	1
1.2 Types of drones.....	3
1.3 Preference of UAV over MAV	3
1.4 Scope of Project	4
1.5 Problem Statement	5
1.6 Objectives	6
1.7 Chapter Organization.....	6
CHAPTER 2 LITERATURE REVIEW	8
2.1 Introduction.....	8
2.2 System Setup.....	8
2.2.1 Electronic Speed Controller (ESC)	10
2.2.2 BLDC Motor	11
2.2.3 Propellers	17
2.2.4 Energy Storage System (ESS).....	20
2.3 System Architecture.....	23
2.4 Quadcopter flight dynamics	25
2.5 Proportional-Integral-Derivative (PID).....	29
2.6 Obstacle avoidance	29
2.6.1 Ultrasonic sensor.....	29
2.6.2 Stereo Vision.....	36
2.7 GPS tracking	38
2.8 Quadcopter Reliability Analysis	41
2.9 Drone for emergency service delivery	44
2.10 Summary	45
CHAPTER 3 METHODOLOGY	47
3.1 Introduction.....	47
3.2 Project Implementation Flow.....	47

3.3	Overall Drone’s Algorithm	48
3.4	Building of hardware - Lists of components.....	49
3.4.1	Navio2 Emlid Flight Controller	49
3.4.2	Raspberry Pi3 Model B.....	50
3.4.3	Airframe.....	51
3.4.4	Motors 2216/950KV	52
3.4.5	Electronic Speed Controller (ESC).....	53
3.4.6	Propellers	54
3.4.7	GNSS receiver with antenna	54
3.4.8	Transmitter.....	55
3.4.9	Receiver	56
3.4.10	MicroSD card.....	56
3.4.11	Lithium-Polymer (Li-Po) Battery	56
3.4.12	Power Module.....	58
3.4.13	Telemetry	58
3.4.14	Assembled quadcopter	59
3.4.15	Thrust-to-weight ratio	60
3.5	System Architecture.....	63
3.6	RPi3 setup and configuration.....	68
3.7	Setting up Ardupilot.....	70
3.8	Flight calibration.....	72
3.9	Obstacle avoidance	73
3.10	GPS tracking	82
3.11	PID control for Quadcopter’s stability.....	84
3.12	Summary	86
CHAPTER 4 RESULTS AND DISCUSSIONS.....		87
4.1	PID tuning	87
4.2	Obstacle avoidance system	96
4.3	GPS tracking in Auto Mode.....	101
4.3.1	First mission – sharp-point turning	101
4.3.2	Second Mission – Around the stadium	106
4.4	Crash Analysis – hardware failure	111
4.5	FPV	113
4.6	Quadcopter Reliability Analysis	115
CHAPTER 5 CONCLUSION.....		120
REFERENCES.....		122

LIST OF TABLES

Table 1.1: Level of autonomous of system	2
Table 1.2: Comparisons between MAV and UAV [20].....	4
Table 2.1: Characteristics of different types of batteries	21
Table 2.2: Quadcopter frame, battery, motor and propeller size matching [36]	24
Table 2.3: Statistical analysis of ultrasonic and infrared sensors' data for different obstacle material [41]	34
Table 2.4: DOP ratings and description [55]	41
Table 3.1: Li-Po battery size based on quadcopter size [36]	57
Table 3.2: Unladen weight of the quadcopter	60
Table 3.3: Datasheet of rotor provided by supplier.....	61
Table 3.4: Thrust estimation based on various parameters [36]	63
Table 3.5: Differences between FHSS and DSSS radio protocol	65
Table 3.6: Flight modes of APM quadcopter [64].....	66
Table 3.7: Roll and pitch override with respect to distance of object detected.....	81
Table 3.8: WP table.....	83
Table 4.1: Effects of increasing PID gains	91
Table 4.2: Responses of quadcopter to different directions of object detected.....	96
Table 4.3: Pitch and roll channel values with respect to distances of object detection.....	99
Table 4.4: Pitch and roll channel values with respect to distances of object detection and direction of detection	100
Table 4.5: Probability of failure guide of component	115
Table 4.6: Severity of failure guide of different component.....	116

LIST OF FIGURES

Figure 1.1: Types of drones based on the airframe design [18][19].....	3
Figure 2.1: Typical system setup schemes of quadcopter using Ardupilot	8
Figure 2.2: Basic component of a typical drone [3].....	9
Figure 2.3: Switching cycle of 3-phase inputs to a motor from an ESC for stator coil excitation.....	10
Figure 2.4: Model of the multirotor propulsion unit [19]	10
Figure 2.5: Types of motors used in UAV applications [26].....	11
Figure 2.6: Structure of a BLDC motor	12
Figure 2.7: Equivalent circuit of each phase of BLDC motor [26].....	13
Figure 2.8: Four-constant model for BLDC motor [6]	14
Figure 2.9: Experimental setup to study the relationship between thrust and motor speed	16
Figure 2.10: Block diagram of the test of physical parameters using PowerLog 6S and Load cell signals and analysis through PC [19].....	17
Figure 2.11: Example of actual and theoretical comparison of graph of thrust (kg) against motor speed (rpm) [10].....	17
Figure 2.12: The pressure and velocity distribution across the length of a propeller disk.....	19
Figure 2.13: Simplified system architecture [21].....	23
Figure 2.14: Quadcopter setup connection with navio2 [35].....	24
Figure 2.15: Roll, Pitch and Yaw – three-dimensional x, y, and z-axis of the quadcopter.....	25
Figure 2.16: Plan view of a quadcopter in lying on its roll-pitch axis	26
Figure 2.17: Movement of quadcopter with respect to motor speed [7]	28
Figure 2.18: Timing diagram of ultrasonic sensor	30
Figure 2.19: Directional uncertainty of an ultrasonic sensor	32
Figure 2.20: Vector computation of distance through anterolateral ranging	33
Figure 2.21: Obstacle avoidance algorithm using ultrasonic sensor.....	35
Figure 2.22: Collision recovery routine for obstacle avoiding robots.....	35
Figure 2.23: Concept of collision avoidance	35
Figure 2.24: The illustration of object taken with two cameras.....	36
Figure 2.25: The illustration of object taken with (a) left camera, (b) right camera.....	37

Figure 2.26: Four-satellite tetrahedron resembling DOP values [53]	41
Figure 2.27: MTBF of military drones.....	43
Figure 2.28: Flowchart of implementation of drone for emergency aid delivery	44
Figure 3.1: Project implementation flow chart	47
Figure 3.2: Overall drone’s algorithm.....	48
Figure 3.3: Navio2 Emlid Flight Controller.....	50
Figure 3.4: Raspberry Pi3 pin connection diagram.....	51
Figure 3.5: Coding for the addition of turn-off switch at free pin 11 or GPIO17 of RPi	51
Figure 3.6: Quadcopter airframe setup (a) Propeller protectors, (b) Power Distribution Board, (c) Rotor arms and central cross arm, (d) Camera or gimbal holder, (e) Carbon- fibre landing gear.....	52
Figure 3.7: Rotor.....	52
Figure 3.8: Electronic Speed Controller (ESC).....	53
Figure 3.9: Balanced propellers	54
Figure 3.10: GNSS receiver and antenna.....	54
Figure 3.11: Radio transmitter	55
Figure 3.12: (a) Receiver, (b) Power Return Module (PRM)	56
Figure 3.13: Graph of various batteries’ (a) volumetric energy density against specific energy density, (b) gravimetric energy density against volumetric energy density [59].....	56
Figure 3.14: Radio telemetry	59
Figure 3.15: Quadcopter after assembly	59
Figure 3.16: The overall circuit connection of the quadcopter	59
Figure 3.17: Overall drone’s system architecture	63
Figure 3.18: Wi-Fi network configuration setting of RPi3	69
Figure 3.19: PuTTY SSH configuration	70
Figure 3.20: Ardupilot greeting interface	70
Figure 3.21: Emlid tool setting	71
Figure 3.22: (a) Telemetry configuration on Navio2, (b) Network IP address.....	72
Figure 3.23: Object detection and avoidance flowchart.....	75
Figure 3.24: Maxbotix ultrasonic sensor connection diagram.....	76

Figure 3.25: Orientation and pin setting of rangefinder.....	76
Figure 3.26: The MaxSonar is not a ratiometric sensor.....	76
Figure 3.27: The type of rangefinder is selected.....	76
Figure 3.28: The maximum and minimum distance for sonar detection is specified	76
Figure 3.29: The type of proximity sensor used is selected.....	77
Figure 3.30: Radar window for object detection.....	77
Figure 3.31: Object avoidance using HC-SR04 ultrasonic sensor.....	78
Figure 3.32: USB to TTL conversion for telemetry air module.	79
Figure 3.33: Ultrasonic sensor model	80
Figure 3.34: Generating WP file through Mission Planner.....	82
Figure 3.35: PID control of the quadcopter	84
Figure 4.1: More overshoots and lesser steady-state error is observed in the vehicle's roll when the proportional gain is too high.	87
Figure 4.2: Higher roll attitudes than desired attitude the control is highly sensitive in higher P gains	88
Figure 4.3: Overshoots reduce significantly when proportional gain is reset to normal, but steady-state error exists before integral responses set in	88
Figure 4.4: Apart from reducing overshoots, roll output has much reduced sensitivity than desired rate when proportional gain is reset to normal.	89
Figure 4.5: Increased or too high a proportional gain can lead to even more severe overshoots and oscillations, though significantly minimises steady-state error.....	89
Figure 4.6: Increased derivative gains optimise sensitivity, reduce overshoot, but has no effect on the steady-state error	90
Figure 4.7: Aptly selected PID gains give moderately sensitive responses, low steady-state error, and no overshoot or oscillations.....	90
Figure 4.8: Gyrosensor data in 3 axes.....	91
Figure 4.9: Accelerometer sensor data in 3 axes	92
Figure 4.10: Gyro sensors bias.....	92
Figure 4.11: The Earth's magnetic field strength.....	93
Figure 4.12: The body fixed magnetic field.....	93
Figure 4.13: Three axes innovations of magnetometer measurements	94
Figure 4.14: Ratio of innovations of GPS velocity	94

Figure 4.15: Ratio of innovations of position and altitude.....	95
Figure 4.16: Ratio of innovations of magnetometer is affected by throttle output.....	95
Figure 4.17: Desired quadcopter roll and pitch during object avoidance testing.....	96
Figure 4.18: Serial monitor of Arduino showing different readings of the ultrasonic sensor for each direction	96
Figure 4.19: Individual test of 1410/1590 pitch roll for 50 cm object.....	97
Figure 4.20: Individual test of 1450/1550 pitch roll for 90 cm.....	97
Figure 4.21: Individual test of 1300/1700 pitch roll for 90 cm object.....	98
Figure 4.22: Mixed test for 1450/1550 for 90 cm detection and 1300/1700 for 40 cm detection	98
Figure 4.23: Final object avoidance pitch-roll response	99
Figure 4.24: Comparison of actual and desired roll.....	100
Figure 4.25: Comparison of actual and desired pitch	101
Figure 4.26: The actual flight path that the quadcopter followed through from KMZ file.....	102
Figure 4.27: A 3D street view image of the flight path of mission one.....	102
Figure 4.28: Plot of latitudinal coordinates throughout the flight of mission one	103
Figure 4.29: Plot of longitudinal coordinates throughout the flight of mission one	103
Figure 4.30: HDOP for GPS	103
Figure 4.31: Number of satellite reception	104
Figure 4.32: Altitude and GPS speed of the quadcopter.....	104
Figure 4.33: Yaw and ground course (GCrs).....	105
Figure 4.34: WPs of flight (a) of the first lap, (b) of the second lap of mission two	106
Figure 4.35: The actual flight path that the quadcopter followed through from KMZ file of mission two.....	106
Figure 4.36: 3D Street view image of the flight paths of mission two	107
Figure 4.37: Plot of latitudinal coordinates throughout the flight of the second mission	107
Figure 4.38: Plot of longitudinal coordinates throughout the flight of the second mission.....	108
Figure 4.39: The intended coordinate of WPs in text file of (a) first lap (b) second lap	108
Figure 4.40: Zoomed-in street view image	108
Figure 4.41: Barometer altitude and GPS speed for stable speed averaged at 3 metre/s	109

Figure 4.42: HDOP for second mission	109
Figure 4.43: HDOP correlation with number of satellites received during the second mission.	110
Figure 4.44: Ground Course from GPS and yaw data	111
Figure 4.45: Desired and actual roll in crash	111
Figure 4.46: Desired and actual pitch in crash.....	112
Figure 4.47: Altitude and throttle output crash	112
Figure 4.48: Abnormal vibrations in flight crash.....	112
Figure 4.49: Motor current draw graph.....	113
Figure 4.50: FPV footage 1.....	113
Figure 4.51: FPV footage 2.....	114
Figure 4.52: FPV footage 3.....	114
Figure 4.53: FPV footage 4.....	114
Figure 4.54: Overall quadcopter failure tree analysis diagram	115
Figure 4.55: Propulsion unit failure tree analysis diagram	115

LIST OF ABBREVIATIONS

ADC	Analog to Digital Converter
AED	Automated External Defibrillator
AHRS	Attitude Heading Reference System
APM	Ardupilot
BLDCM	Brushless DC Motor
CA	Criticality Analysis
DAU	Data Acquisition Unit
DCA	Department of Civil Aviation
DCM	Direction Cosine Matrix
DHCP	Dynamic Host Configuration Protocol
DoD	Depth of Discharge
DOP	Dilution of Precision
DSSS	Direct Sequence Spread Spectrum
EKF	Extended Kalman Filter
EMF	Electromotive Force
EMS	Emergency Medical Service
ESC	Electronic Speed Controller
ESS	Energy Storage System
FC	Flight Controller
FHSS	Frequency Hopping Spread Spectrum
FMEA	Failure Mode and Effect Analysis
FOC	Field-Oriented Control
FPV	First Person View

FTA	Failure Tree Analysis
GCrs	Ground Course
GCP	Google Cloud Platform
GCS	Ground Control Station
GDOP	Geometric Dilution of Precision
GNSS	Global Navigational Satellite System
GPIO	General Purpose Input Output
GPRS	Global Packet Radio Service
GPS	Global Positioning System
GSM	Global System for Mobile Communication
GUI	Graphical User Interface
HDD	Hard Disk Drive
HDOP	Horizontal Dilution of Precision
HTFP	High Throughput Field Phenotyping
IDE	Integrated Development Environment
IMU	Inertia Measurement Unit
IP	Internet Protocol
IPM	Interior Permanent Motor
ITS	Intelligent Transport System
LAN	Local Area Network
LED	Light-Emitting Diode
Li-Po	Lithium-Polymer
LOA	Level of Autonomous
MAV	Manned Aerial Vehicle

MCX	Micro axial
MEMS	Micro-Electro-Mechanical System
MP	Mission Planner
MTBF	Mean Time Between Failure
MTTF	Mean Time to Failure
MTTR	Mean Time to Repair
NOOBS	New Out of the Box Software
OBC	On-Board Computer
ONN	Convolution Neural Network
OS	Operating System
PID	Proportional-Integral-Derivative
PPM	Pulse Position Modulation
PRM	Power Return Module
PWM	Pulse Width Modulation
RC	Radio Communication
RORI	Return of Reliability Investment
RPi 3	Raspberry Pi 3
RTL	Return to Launch
RX	Receiver
SBAS	Satellite Based Augmentation System
SBUS	Serial Bus
SMS	Short Message Service
SoC	State of Charge
SoH	State of Health

SONAR	Ultrasonic Sensor
SPS	Standard Position System
SSD	Solid State Drive
SSH	Secure Shell
SSM	Split System Model
TDOP	Time Dilution of Precision
TTL	Transistor-Transistor Logic
TX	Transmitter
UART	Universal Asynchronous Receiver-Transmitter
UAS	Unmanned Aerial Aircraft System
UAV	Unmanned Aerial Vehicle
USB	Universal Serial Bus
VDOP	Vertical Dilution of Precision
VTOL	Vertical Take-Off and Landing
WP	Way Point

PEMBANGUNAN DRON AUTONOMI UNTUK PELBAGAI FUNGSI

ABSTRAK

Drone autonomi boleh menjalankan fungsi seperti penghantaran bantuan kecemasan, penghantaran bungkusan atau kerja-kerja pemantauan dan penyelenggaraan serta dijadikan alat penyelamat dan penghantaran barangan kecemasan melalui sistem kedudukan global (GPS), seiring dengan sensor untuk sistem penghindaran objek. Tesis ini mengutarakan UAV dan mekanisme yang berfungsi untuk membolehkan penerbangannya, dan turut menjelaskan fungsi yang berbeza sebagaimana dron autonomi direka untuk dilaksanakan, melakukan analisis data penerbangan dari log data dengan menggunakan “Mission Planner” (MP) dan “Google Earth pro”. Yang turut disertakan ialah cara objektif yang berbeza - termasuk membina model UAV dengan mempertimbangkan komponen yang serasi, penghindaran objek menggunakan sensor HC-SR04 atau “Maxbotix” ultrasonik dengan “Arduino IDE”, pengesanan GPS masa nyata dron dengan perisian “Ardupilot” (APM) - dicapai dengan keupayaan teknologi semasa. Dron memanfaatkan “Raspberry Pi 3” (RPi3) sebagai pemproses dan pengawal penerbangan, “Navio2” daripada “Emlid” untuk mengendalikan penerbangannya. Navio2 adalah pengawal penerbangan (FC) canggih yang dilengkapi Unit Pengukuran Inertia (IMU) untuk membekali data penerbangan masa nyata ke FC dan Stesen Kawalan Penerbangan (GCS). Alat penerima GPS menerima isyarat satelit untuk menentukan lokasi UAV, membantu penerbangan UAV melalui titik jalan (WP) dalam mod auto, dan mengetepikan parameter penerbangan yang tidak tepat melalui Penapis Kalman Lanjutan (EKF). Dengan adanya telemetri udara, data penerbangan boleh dipantau melalui GCS tanpa perlunya sambungan rangkaian kawasan setempat (LAN). Sehubungan dengan itu, komunikasi radio (RC) dan rangkaian yang protokol yang bersesuaian perlu untuk menghubungkan alat penghantar dengan alat penerima supaya komunikasi antara pelbagai peranti dapat diwujudkan. Dron ini mempergunakan pemancar dan penerima 12 saluran AT10-II dari RadioLink Electronics untuk pengendalian manual atau peralihan operasi berautonomi. Analisis kebolehpercayaan dron dijalankan berdasarkan analisis keberangkalian kegagalan komponen dan analisis tahap kritikal. Dron yang dibina telah berjaya menjalani penerbangan autonomi yang dilengkapi sistem penjejakan GPS dan sistem perancangan perjalanan, serta keupayaan untuk menghindari objek dengan pergerakan lanjutan yang bersesuaian dengan jarak pengesanan objek.

DEVELOPMENT OF AUTONOMOUS DRONE FOR MULTI-PURPOSE FUNCTIONS

ABSTRACT

Autonomous drones can carry out functions such as emergency aid delivery, parcel delivery or inspection works with the help of global positioning system (GPS) location tracker, along with sensors for object avoidance. This thesis provides understanding of UAV and the mechanisms that work together to enable its flight, elaborates the different functions that the autonomous drone is designed to carry out, performs flight data analysis from flash logs on Mission Planner (MP) and Google Earth, and discusses how different objectives – including building the UAV model by considering suitable hardware, object avoidance using HC-SR04 or Maxbotix ultrasonic sensor with Arduino IDE, real-time GPS tracking of drone with Ardupilot (APM) software – are achieved with the current state of technology. The drone uses Raspberry Pi (RPi3) as the processor and a stackable flight controller, Navio2 by Emlid to control its flight. Navio2 is a well-documented, latest developed flight controller (FC) by Emlid, with an array of built-in sensors to assist through different autopilot missions. Advanced Inertial Measurement Unit (IMU) feeds real time flight data to the processor as well as the Ground Control Station (GCS). Global Navigational Satellite System (GNSS) receiver accepts satellites' signal to pinpoint location of UAV, assist the UAV's flight over waypoints (WP) in auto modes, and override inaccurate flight parameters through Extended Kalman Filter (EKF). With an external 915 MHz radio telemetry in place flight data can be monitored from GCS even without the need of a Local Area Network (LAN) connection. The drone utilises a 12-channel AT10-II RC transmitter and receiver pair by RadioLink Electronics to enable manual or semi-autonomous control and initiation operations of autonomous mode. A reliability study of the drone is carried out based on failure tree and criticality analysis. The drone is successfully set on mission on GPS tracking and path planning in autonomous mode and is able to respond to obstacles in the object avoidance mode with suitable pitch and roll values based on detected distances.

CHAPTER ONE

INTRODUCTION

1.1 Background

Drone emerges as the best alternatives for numerous operations [1-5] including search and rescue, emergency service delivery, parcel delivery, maintenance, agriculture, surveillance, manufacturing, or even military [6-10]. They are commonly seen to send aids to drowning victims, recognising distress signals through machine learning and image processing, and being a substitute to an ambulance as the first-to-arrive medical service, sending first aids or Automated External Defibrillator (AED) before the arrival of skilled paramedics.

Drones also can be human substitutes for search and rescue operations [10-12], where live video streaming through cameras can provide real-time information to a control centre. Thermal cameras can detect human presence from far and accurately locate through GPS humans who gets lost in deserts. Through machine learning, drones can even be trained to recognise and distinguish distress signals such as waving and SOS signs before triggering distress calls to a control centre.

Drones can be used as a tool for parcel delivery [3]. Local goods delivery through drones has been launched by Amazon on 7th December 2016 through the project named Prime Air. The deliveries were successful and are expected to expand. With GPS, parcels can be delivered precisely to predefined locations. This prominent success assures us that drones will revolutionise the supply chain industry, and this is partly attributable to the reduce of fuel and labour cost, improvement of customers' satisfaction, and the rise of operational efficiency and productivity [13].

Talking about industry, drones have had truly remarkable performances in delivering precise works such as inspection of overhead grids or cables, carrying out simple maintenance works or delivering parts for assembly in the manufacturing line. Drone will certainly be an indispensable companion in most of the industries in the near future.

In terms of agricultural and geographical mapping [6], drones also play a crucial part in field supervision [3]. Responses of agricultural growths to droughts can be

effectively studied with UAV-based thermal imaging. High-throughput field phenotyping (HTFP) is the highly precise, efficient and non-destructive screening of genotype performance in plantations [14].

Autonomous drones are those which are able to optimise their behaviour in goal-oriented manners during unforeseen situations. They should be able to react to external stimulus without requests or guidance from the operators [15]. This is different from automatic systems, which are fully pre-programmed according to fixed rules regardless of all kinds of situations [16]. The level of autonomous (LOA) of systems can be categorised according to the Table 1.1.

Table 1.1: Level of autonomous of system

LOA	Meaning
1	Human makes all decisions
2	Computer computes complete set of alternatives.
3	Computer chooses a set of alternatives.
4	Computer suggest one alternative.
5	Computer executes suggestion with approval.
6	Human can veto computer's decision within timeframe.
7	Computer executes, then reports to human.
8	Computer only reports if asked.
9	Computer reports only if it wants to.
10	Computer ignores the human.

Object avoidance of the drone in this project is a 6th level of autonomous (LOA) in the LOA scale provided by Parasuraman, Sheridan et al [17], in which computer generated pitch-roll can be overridden by human interference through a radio transmitter. Similarly, even when the quadcopter is pursuing specific Waypoints (WP), the pilot can take control of the flight anytime he feels necessary. This ensures that the project developed is in compliance with the local aviation regulations by the Department of Civil Aviation (DCA).

1.2 Types of drones

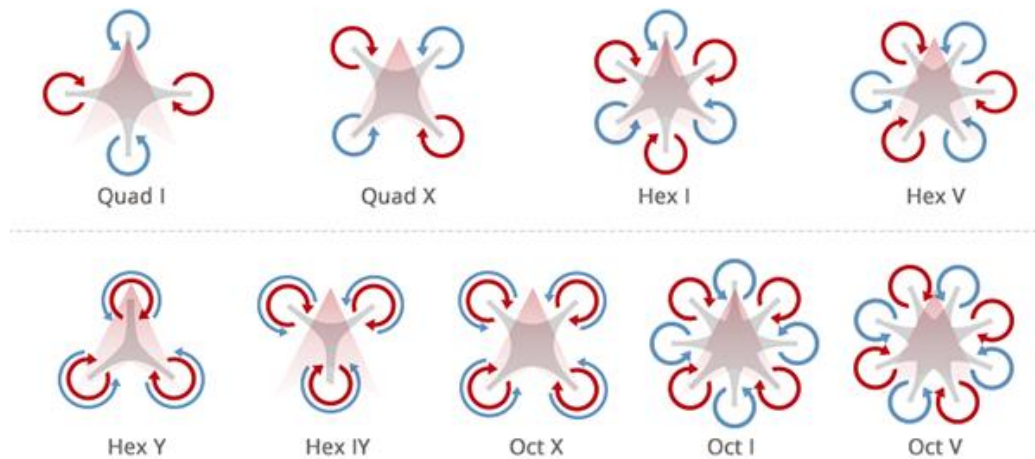


Figure 1.1: Types of drones based on the airframe design [18][19]

Drones come in a variety of sizes and types. Types of drones can be classified according to the number of rotors. A single-rotor drone is a mini drone, light-weight and flies with only one propeller. With disadvantages in terms of stability, single-rotor drones are replaced by the more common tricopters or hexacopters with 3 and 4 rotors respectively. Both of these drones can be trick drones or prosumer drones and payloads can be attached to the base of the drone. Hexacopters or octocopters are much more complex drones designed to lift heavy payloads at excellent stability for professional photography or cinematic actions [18]. As shown in Figure 1.1, each type of drones has its universal set of direction of rotation for each of its rotor, with the common aim to balance airflow and provide thrust as the motor accelerates. The UAV used in this project is the Quad X airframe for optimum performance and safe landing.

1.3 Preference of UAV over MAV

Manned Aerial Vehicles (MAV), unlike UAV, requires an on-board pilot to control the aircraft. MAV are often helicopters that operated by authorised skilled personnel to execute certain duties.

Nevertheless, MAV incurs high investment and operational costs, and risks lives carrying out challenging tasks [10]. Recently, Unmanned Aerial Vehicle (UAV), or Unmanned Aerial Aircraft System (UAS) has proved an essential substitute for MAV,

making them a game changer in many applications including the Intelligent Transportation System (ITS) infrastructure [20]. The comparison between MAV and UAV is as shown in Table 1.2.

Table 1.2: Comparisons between MAV and UAV [20]

Aspects	MAV	UAV
Length coverage	High	High
Security/Privacy	Medium	Low
Cost (acquiring and maintenance)	High	Low
Multiple uses	High	High
Energy Efficiency	Low	High
Deployment	Low	High
Operation time	High	Low
Operation in adverse weather	Low	Low
Risk	High	Medium
Endurance	High	Low
Video post-processing skills	High	High
Data transfer, communication and storage	High	High
Operation skill	High	Medium
Training requirement	High	Medium
Complexity	High	Medium

1.4 Scope of Project

The scope of this project revolves around the development of an autonomous drone for a variety of functions. Hardware assembly is the first step of the drone's overall development. Different components have to be studied and selected accordingly based on the design requirement of the project.

The installation of FC follows suit, with the Raspberry Pi3 microcomputer set up, configured and mounted with the Navio2 FC. The IMUs of the drone are initialised and calibrated before the tuning is carried out.

Obstacle avoidance requires the use of components such as ultrasonic sensor (SONAR), to be installed to the drone. Sonar detects distance ahead using the reflection of sound waves and initiate a response to sway away from nearing obstacles.

The location tracking ability of the drone means that the drone has to rely on GPS receiver readily built into the FC. Different GCS software are able to provide mission planning or path planning whereby the drone can, with functional GNSS or GPS receiver and low Dilution of Precision (DOP) values, follow suit a pre-planned path on Google Map interface.

Analysis of different flight data tells more for flight quality improvement and reliability analysis contributes to the enhancement of overall system quality.

1.5 Problem Statement

Although drones are set on a journey to revolutionise the industry, many limitations of drone to complete missions require researches. Firstly, drones have limited flight time when they involve electric propulsion. The right capacity of battery with respect to the drone's size and overall weight needs to be used. Drones are also known to have caused accidents because most drones do not incorporate autonomous functions and obstacle avoidance due to high implementation cost. Researches on autonomous functions and object avoidance using more commonly available and low cost sensors are needed as the key toward widespread availability of object avoidance for safer drones in all kinds of functions.

Drones are multipurpose and can be a human substitute in risky operations. Human errors, topographical aspects, manpower limitations, risks, and unfavourable conditions [21] are some of the reasons why drones can be particularly helpful to offer help. Drones emerge in limitless applications and the demand for related researches and studies are now in need for overall system and feature's enhancement as well as cost reduction for wide-spread commercialised usages.

1.6 Objectives

The objectives of this project are:

1. To assemble and build a quadcopter using all hardware and components required.
2. To implement object avoidance on the built quadcopter using suitable distance sensors.
3. To implement GPS tracking and mission or path planning using available GCS that supports Google Map.
4. To perform a simple reliability analysis of the built quadcopter using failure tree analysis with criticality analysis.

With the objectives of the project listed achieved, the autonomous drones can serve a multiple variety of functions such as emergency first aid delivery, First Person's View (FPV) for inspection works, as well as parcel delivery. These can be only be done with the achievement of the first three objectives stated. The fourth objective analyses the flight of the built prototype as results for practical understanding and future improvements.

Analysis on data of flights on a variety of purposes, such as on object avoidance, auto mode or GPS tracking, or ordinary flight control will be carried out using data flash log on Mission Planner or Google Earth.

In this project, the autonomous drone should be able to fly to defined locations with GPS tracking, while avoiding obstacles that arise in its path.

1.7 Chapter Organization

This report consists of three chapters. Chapter 1 provides introduction to the project including the background of the project, problem statement, objectives, and the scope of the project.

Chapter 2 records literature reviews which describe possible ways different parts of the projects can be carried out based on available published researches, for example, the building of the drone, motors and ESC, propellers, battery, obstacle avoidance, GPS tracking, communication protocols and the design of the UAV.

Chapter 3 presents methodology of this project. In this chapter, the concepts and algorithm for the drone's development are discussed and explained in detail, based on the objectives stated. The methodology describes in steps how the drone is being built, set up and configured, how object avoidance is implemented in the drone, how GPS tracking is used to help achieve path or mission planning, how flight data is analysed and used for flight stability improvement, and how the reliability of the drone is being analysed through failure analysis.

Chapter 4 explains in detail the results and discussions of the project implementation using ingredients in Chapter 2 and methodology in Chapter 3. The results are supported with visuals and illustrations as well as inferences drawn to explain the obtained results. Analysis of flights for PID tuning, testing of object avoidance system and GPS tracking of the quadcopter are being elaborated in depth. The quadcopter's crash and reliability analyses are carried out to improve overall drone's safety and reliability.

Chapter 5 provides a conclusive summary of the entire project implementation which included introduction, literature review, methodology, results and discussions.

CHAPTER TWO

LITERATURE REVIEW

2.1 Introduction

UAV has been in the research area for the development of tools for repetitive, complex or high-risk works [22][23]. It is favoured due to its high maneuverability, speed, precision and limitless applications it can be involved with [2]. Drone is a type of UAVs which provides even greater manoeuvrability with VTOL, and can hover at a desired location [2][13][21][22].

Being the most common type of VTOL aerial vehicle, a quadcopter uses 4 propellers for lift and stabilisation. The rotors are placed in a square or diamond shape in equal distance from the frame's mass centre. By adjusting the angular velocities of the rotors the quadcopter can be controlled [24].

2.2 System Setup

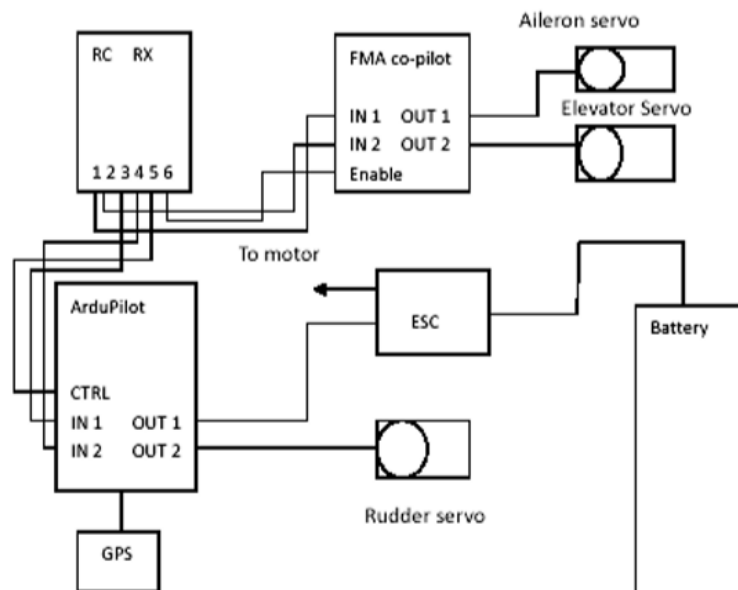


Figure 1.2: Typical system setup schemes of quadcopter using Ardupilot

System setups of drones can be referenced from different sources[1][22], but the main concept and hardware do not differ much [19]. Figure 1.2 shows the fundamental component circuit diagram of typical UAV with embedded processor called Ardupilot.

Figure 1.3 shows that the 5 main components that make up a drone are the FC, ESC, battery, payload and sensors [3]. To fly a drone in the manual mode, a radio receiver and transmitter pair will be required.

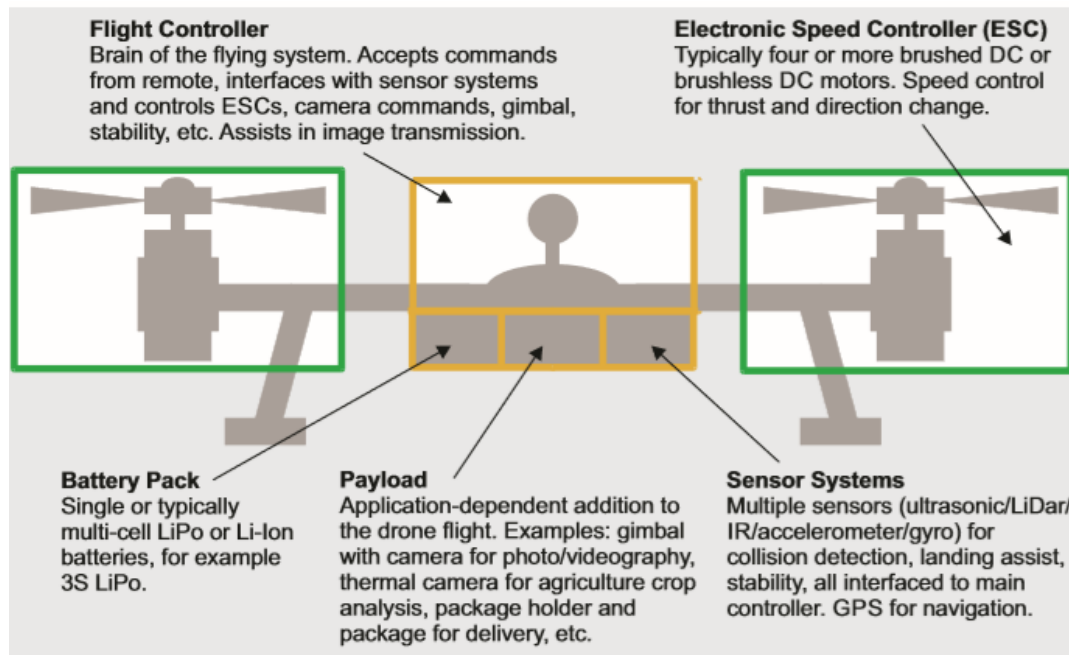


Figure 1.3: Basic component of a typical drone [3]

Otherwise, a drone can fly on its own without a pilot, through the autopilot mode [7]. This requires more advanced FCs, one of which is ArduPilot, a full-featured platform based on the open-source Arduino platform. It is a custom printed circuit board (PCB) with an embedded processor combined with circuitry to control desired output [15], and to switch between RC control and the autopilot control. Autopilot controls navigation with GPS and Waypoints (WP) following as well as altitude control by controlling the rudder, elevator and throttle [1].

The propulsion unit is also a fundamental component that consists of an ESC, a motor and a propeller. Motor control can either be closed loop or open loop [3]. Closed loop control has sensed motors to estimate rotor angle, and to test if the rotor is moving as expected. If not, the control loop will automatically increase or reduce current supply as per required. The sensor used for rotor position is often a Hall Effect sensor [25], whose operation cycle with respect to back-EMF of motors are as shown in Figure 1.4. Sensorless field-oriented control (FOC) uses three-phase voltage to calculate rotor angle. Therefore, overshoots are common in speed control of sensorless FOC, but are often

minimised when propellers are in place to compensate speed inertias with air resistances [3].

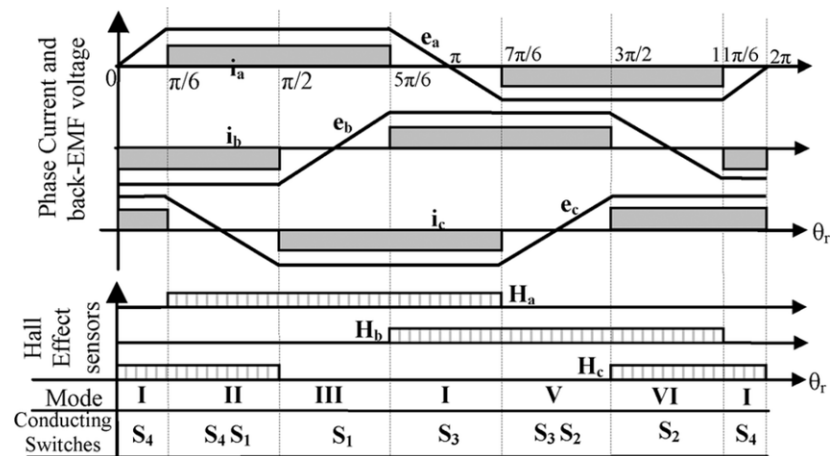


Figure 1.4: Switching cycle of 3-phase inputs to a motor from an ESC for stator coil excitation

2.2.1 Electronic Speed Controller (ESC)

The electric propulsion system, as shown in Figure 1.5, converts electrical energy from the battery to mechanical power in the form of thrust through the ESC [6][10]. The ESC receives PWM throttle control signal from the FC, which – if not in the autopilot mode – in turn receives inputs from the radio receiver [6]. As shown in Figure 1.3, the ESC has built-in or integrated inverter or switching supply that produces three phase AC output, or in other words 3-phase bi-directional square wave to the Brushless DC motor (BLDC). The duty cycle of each of the chopped supply voltage determines the speed of the motor [19].

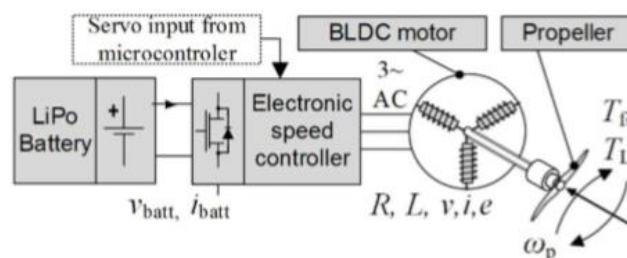


Figure 1.5: Model of the multirotor propulsion unit [19]

The ESC rating has to be higher than the maximum ampere rating of the motor to prevent overheating [10][17] as shown in equation 2.1.

$$ESC \text{ Rating} = (1.2 \text{ to } 1.5) \times \text{Maximum Motor Ampere Rating} \quad (2.1)$$

The ESCs are supplied with DC bus voltage ranging from 7.4 V to 22.4 V with DC current link from the Li-Po generally ranges from 10 A to 20 A. PWM module of ESC has desired frequency between 30kHz to 60kHz to avoid interference with on-board sensors [3].

2.2.2 BLDC Motor

There are many types of electric motors which may be suited for UAV applications, some of which are shown in Figure 1.6.

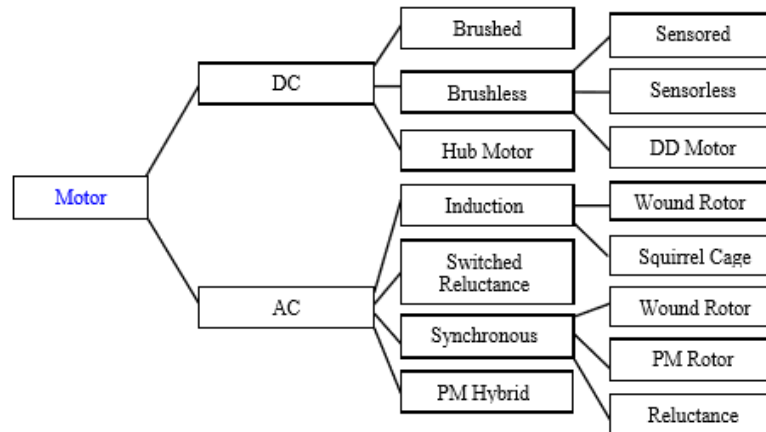


Figure 1.6: Types of motors used in UAV applications [26]

Brushless DC motors (BLDC motors) or the trapezoidal back electromotive force (Back EMF) motor is a synchronous machine [4] that offers several advantages to suit UAV applications. These advantages include high torque to weight ratio, being commutatorless and brushless [4][25][26], having smaller size, reduced noise, reduced maintenance, increased reliability, increased lifetime and efficiency [10].

The ESC translates the PWM to variable percentage duty cycle of a quasi-three-phase AC power to the BLDC motor, given by

$$P_{esc} = V_{esc} \times I_{esc} \quad (2.2)$$

Where:

P_{esc} = Power of ESC

V_{esc} = Voltage across ESC

I_{esc} = Current of ESC

This can be seen through the 3 wire connection of the BLDC to the ESC output, as shown in Figure 3.8. With the quasi-three-phase AC power output from the ESC, these 3 wires powers up 3 separate pairs of opposite coils in the BLDC at alternate times according to the switching sequence determined by the ESC as shown in Figure 1.4. The graph shows the back-EMF for BLDC motors being trapezoidal, which differs from the sinusoidal phase voltage of in Brushless AC (BLAC) motors [3]. Trapezoidal control leads to current spikes and commutation ripples that cause vibrations, but requires less controller performance [3].

To understand why and how BLDC motors are powered by an AC supply, understanding on the working principle of BLDC is a prerequisite. As shown in Figure 3.7, a BLDC motor consists of a pair of permanent magnets [27] at the outside as its rotor and 3 pairs of excitable coils in the centre as its stator. In order to make the rotor turns, the coils have to be magnetised in a way – as shown in Figure 1.7 – that the permanent magnetic poles are always repelled by its corresponding stator coil, and attracted toward the next coil in place in the direction of rotation. In the usual operation, 2 pairs of coils will be energised at each switching interval to increase power output and torque consistency.

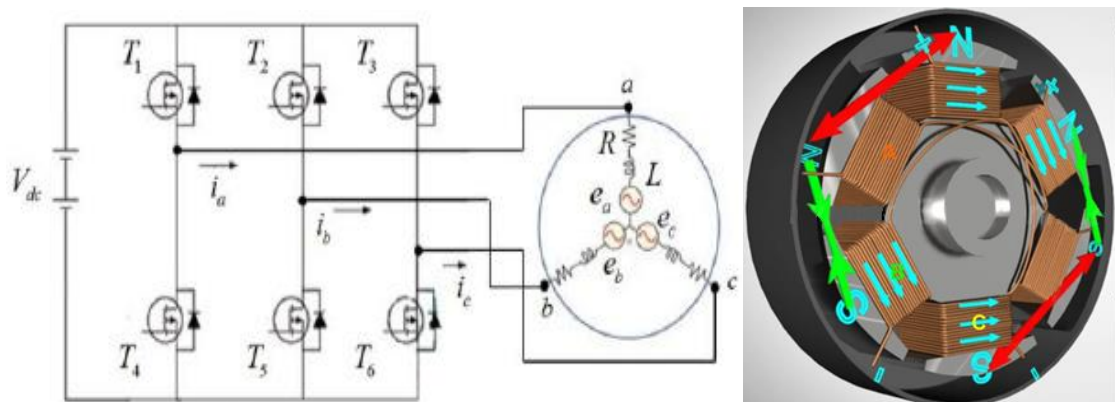


Figure 1.7: Structure of a BLDC motor

This type of BLDC can be called an outer rotor BLDC motor [27] or out-runner BLDC motor [28]. In-runner BLDC motors, or embedded interior permanent magnet (IPM) motors, on the other hand, despite having better torque performance, have lower mechanical integrity to support high speed applications like those in a quadcopter [27] [28]. Performance-wise, BLDC motor with non-linear speed control response is shown to have better flight-path tracking and overall performance [28].

The 3-phase outputs from ESC have each phase energising a pair of coils. Each coil in a pair is wound in an orientation according to the Right Hand Grip rule that current flow will induce an opposite magnetic pole to its corresponding counterpart. This is shown clearly in Figure 1.7. Note that for the repel-attract magnetic reaction to take place continuously, the direction of current flow has to be changed or inverted in the next half cycle of alternation [26]. This alternating magnetic pole is simply achieved with the nature of an AC current.

Most BLDC in UAVs are delta-connected for high speed over torque applications. Each phase of the BLDC can be represented with the equivalent circuit as shown [26].

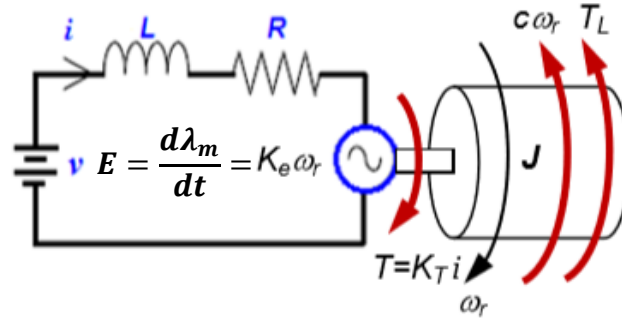


Figure 1.8: Equivalent circuit of each phase of BLDC motor [26]

From Figure 1.8, the electromagnetic torque can be derived as [26]

$$\tau_{em} = \frac{P_{em}}{\omega_r} = \frac{m\omega\lambda_m I}{\omega_r} \quad (2.3)$$

Where:

P_{em} = Electromagnetic output power = $m\omega\lambda_m I$ (W)

m = Number of phases

$\lambda_m = \int E dt$ = Flux linkage of the stator winding per phase induced by the permanent magnet

$\omega = 2\pi f$ = angular frequency (rad/s)

ω_r = Rotor speed (rad/s)

I = Current (A)

Since

$$\omega_r = \frac{2\omega}{p} \quad (2.4)$$

Where:

p = Number of poles

Equation 2.3 can be rewritten as [25][26]

$$\tau_{em} = \frac{mp\lambda_m I}{2} \quad (2.5)$$

The shaft output load

$$\tau_{load} = \tau_{em} - \tau_{loss} \quad (2.6)$$

Where:

τ_{loss} = Torque losses due to friction, iron hysteresis and windage losses

The induced EMF voltage

$$E = \frac{p}{2} \lambda_m \omega_r \quad (2.7)$$

Where:

E = Voltage across the rotor winding

From the equivalent circuit in Figure 1.8, since $\omega L \ll R$,

$$V = IR + E \quad (2.8)$$

Where:

V = Battery supply voltage

Substituting equation 2.5 with I as the subject into equation 2.8, and then substitute equation 2.7 into the new equation formed

$$\tau_{em} = \frac{m \left(\frac{p\lambda_m}{2} \right)^2}{R} \left(\frac{V}{\frac{p\lambda_m}{2}} - \omega_r \right) \quad (2.9)$$

Where:

R = Rotor winding resistance (Ohm)

Equation 2.9 can be written with the rotational speed (rad/s) as the subject [25]

$$\omega_r = \frac{V}{\frac{p\lambda_m}{2}} - \frac{R}{m \left(\frac{p\lambda_m}{2} \right)^2} \tau_{em} \quad (2.10)$$

The BLDC motor model can also be modelled with the four-constant equivalent circuit as shown in Figure 1.9 [6]. From Figure 1.9,

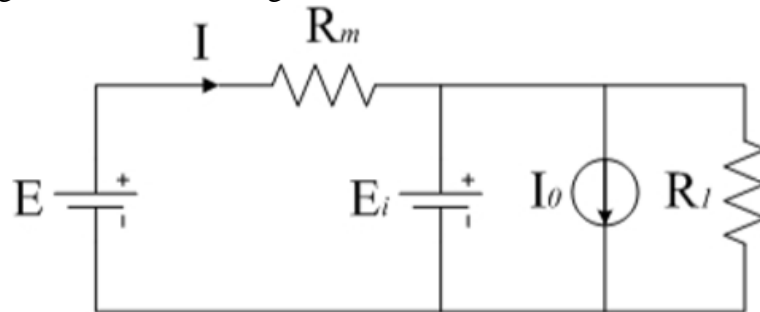


Figure 1.9: Four-constant model for BLDC motor [6]

$$E_i = E - IR_m \quad (2.11)$$

Where:

E_i = Back EMF (V)

E = Battery voltage (V)

I = Battery current (A)

R_m = Combined winding and ESC resistance (Ohm)

The rotational speed of the motor is proportional to the back EMF, E_i with proportionality constant K_v [6][10].

$$K_v = \frac{N}{E_i} \quad (2.12)$$

Where:

K_v = RPM/volt proportionality constant

N = Motor speed (rpm)

E_i = Back EMF (V)

The windage and Eddy current losses, in Ω , of BLDC motors can be computed as [6]

$$R_1 = \frac{E - I(R_{esc} + R_m)}{I - I_0} \quad (2.13)$$

Where:

R_{esc} = ESC resistance

R_m = Winding resistance

I_0 = Current value when the battery current and battery voltage graph intersects

The overall efficiency of a BLDC motor [6]

$$\eta = \frac{P_{load}}{P_{batt}} \times 100\% = \frac{E_i I_i}{E_{batt} I_{batt}} \times 100\% \quad (2.14)$$

Where:

E_i = Back EMF (V)

I_i = Load current (A)

E_{batt} = Battery voltage (V)

I_{batt} = Battery current (A)

$P_{batt} = V_{batt} I_{batt}$ (W)

The efficiency can also be defined by the equation [26]

$$\eta = K \frac{0.7457 P_h L}{P_i} \quad (2.15)$$

Where:

η = Efficiency

P_h = Rated horsepower (hp)

P_i = 3-phase power (kW)

L = Output power as percentage rated power

K = Efficiency correction power

A test [10] has been developed to study the relationship between the motor rpm and the thrust generated. The thrust produced by the rotor is transferred through a lever to a horizontal arm, whose end is weighted and weighed on a scale. The difference in the weighing scale can tell the thrust, and a tachometer is used to measure the BLDC motor's rpm. Theoretical thrust calculated from equation 2.36 can be compared with that of the measured motor thrust. The result is plotted in a graph as shown in Figure 1.12.

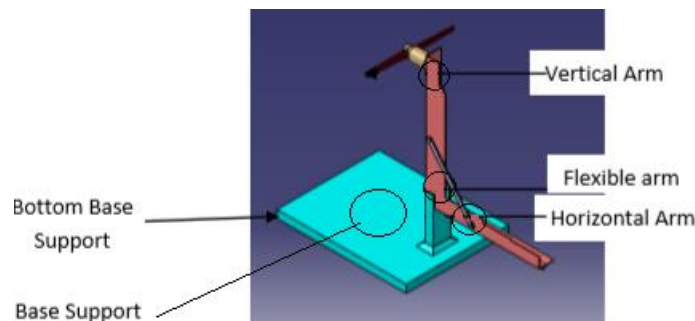


Figure 1.10: Experimental setup to study the relationship between thrust and motor speed

Otherwise, physical parameters for propulsion can be conducted using a load cell type sensor to measure aerodynamic forces and a multifunctional logging meter, PowerLog 6S to measure angular velocity and power consumption. The PowerLog 6S can be integrated with computer, and provide motor voltage measurement as well as non-contact optical sensing of motor rpm. Signals from load cell are amplified and converted from analog to digital through HX711 Analog to Digital Converter (ADC), processed in Atmel ATxmega microcontroller, before fusing with that of the log meter, and captured using the LogView studio software or analysed through MATLAB [19].

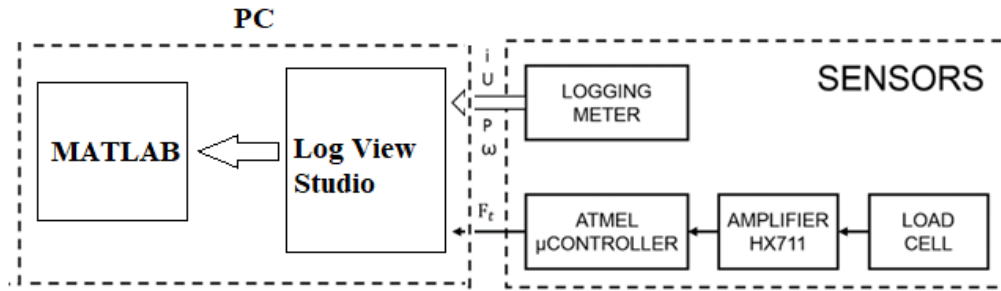


Figure 1.11: Block diagram of the test of physical parameters using PowerLog 6S and Load cell signals and analysis through PC [19]

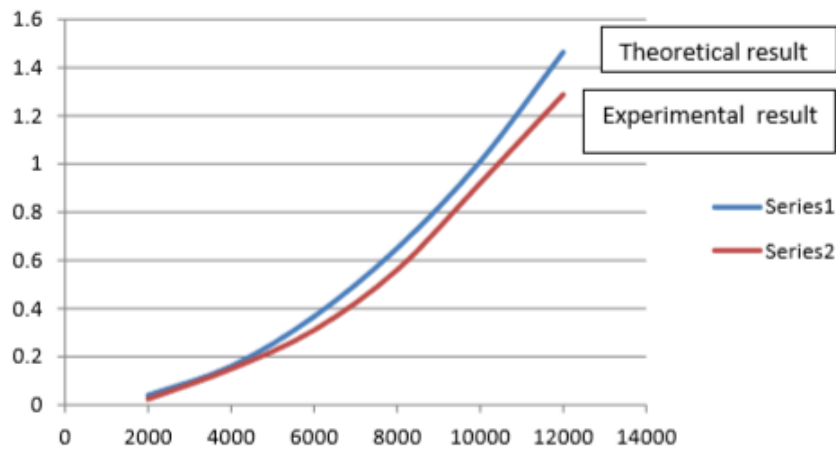


Figure 1.12: Example of actual and theoretical comparison of graph of thrust (kg) against motor speed (rpm) [10]

2.2.3 Propellers

The propeller converts the torque and rotational speed to an aerodynamic thrust. A high KV (or K_v) motor is suited for smaller sized propellers, while lower KV motor uses larger propellers [10]. This simple rule of thumb minimises the burning out of motors due to excessive air resistance when using oversized propellers with high KV motors, or insufficient thrust when using undersized propellers with low KV motors.

Each rotor and its respective propeller is called a propulsion unit. The thrust produced by each propulsion can be calculated from [19]

$$T = k_f \omega^2 = C_T \rho A r^2 \omega^2 \quad (2.16)$$

Where

ω = angular speed of rotor

$k_f = \text{thrust force factor} = C_T \rho A r^2$

$C_T = \text{Thrust coefficient}$

$\rho = \text{Air density}$

$A = \text{Area of propeller disk}$

$R = \text{Propeller radius}$

Drag moment of a propulsion unit

$$\tau = k_\tau \omega^2 = C_P \rho A r^3 \omega^2 \quad (2.17)$$

Where

$\omega = \text{angular speed of rotor}$

$k_\tau = \text{drag torque factor} = C_P \rho A r^3$

$C_P = \text{Power coefficient}$

$\rho = \text{air density}$

$A = \text{Area of propeller disk}$

$r = \text{Propeller radius}$

The thrust coefficient, C_t , power coefficient C_P , and efficiency of a propeller are defined from equation 2.18 to 2.20 [25].

$$C_t = \frac{F_t}{\rho n^2 D^4} \quad (2.18)$$

$$C_P = \frac{Q}{\rho n^3 D^5} \quad (2.19)$$

$$\eta = \frac{C_t J}{C_P} \quad (2.20)$$

Where:

$N = \text{rotational speed}$

$D = \text{diameter of propeller}$

$\rho = \text{air density}$

$F_t = \text{propeller thrust}$

$J = \text{Advance ratio}$

The pressure and velocity distribution across the length of a propeller is shown in Figure 1.13 [25].

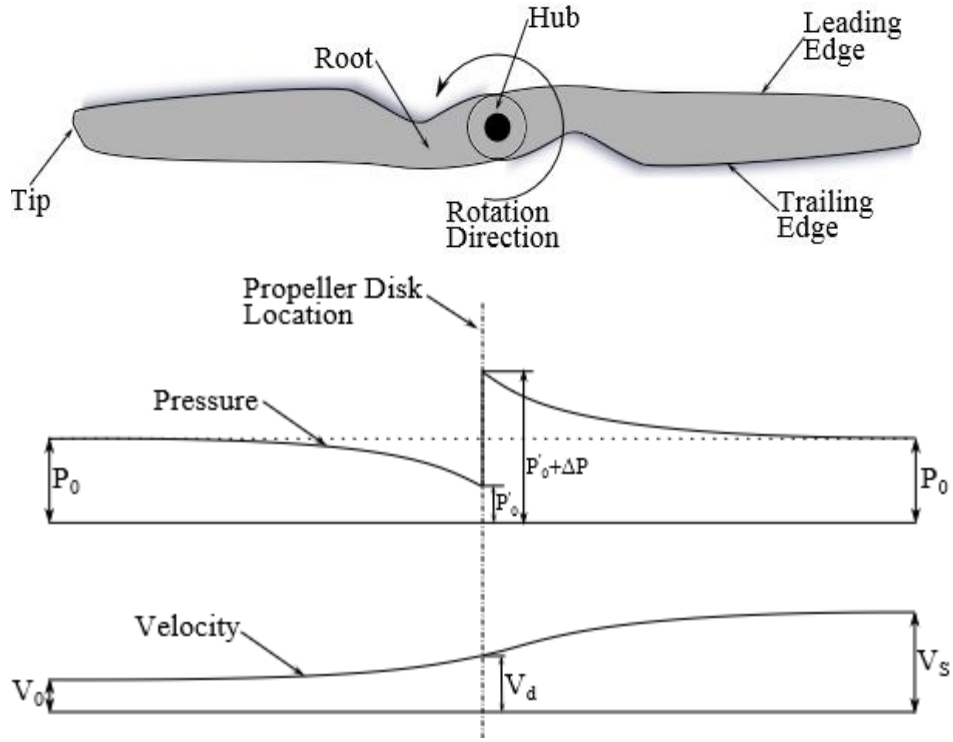


Figure 1.13: The pressure and velocity distribution across the length of a propeller disk

With velocity of air V_0 and V_s , the propeller thrust, F_t can be computed using equations

$$F_t = A_p V_d (V_s - V_0) \quad (2.21)$$

OR

$$F_t = A \Delta P = \frac{A \rho}{2} (V_s^2 - V_0^2) \quad (2.22)$$

Where

$$V_d = \frac{V_s + V_0}{2} \quad (2.23)$$

And in terms of efficiency [25],

$$F_t = 2 \rho V_0^2 \frac{1 - \eta}{\eta^2} \quad (2.24)$$

Where:

$A_p V_d$ = mass per unit time through the disk

$V_s - V_0$ = Velocity increase from far upstream to far downstream

η = propeller efficiency

V_d = propeller disk velocity

V_s = upstream velocity

V_o = downstream velocity

A = Propeller disk area

The propeller efficiency can also be derived as [25]

$$\eta = \frac{E_{out}}{E_{in}} = \frac{F_t V_o}{K.E.} = \frac{F_t V_o}{\frac{1}{2} A \rho V_d (V_s^2 - V_o^2)} = \frac{2}{1 + \frac{V_s}{V_o}} \quad (2.25)$$

Where:

K.E. = Kinetic energy

Blade pitch is an important parameter of a propeller. It is in effect how much air is cut by the blade during the flight. A propeller blade can be well pitched for purpose of cutting more air for lifts during taking off, but that, however, will compromise the maximum horizontal speed of quadcopter [5]. In light of this, variable pitch propellers are now becoming a new line of research to further improve stability for take-offs, landing, as well as during flights [5].

Propeller noise is also an internationally concerned parameters to improve on. Loud noises produced from large UAVs used for marine mammal research has proven to cause disturbances on certain marine mammals such as sea otters and pinnipeds [29]. Propeller noise can be reduced by preventing multiple propellers to rotate in phase [30].

2.2.4 Energy Storage System (ESS)

Numerous studies and attempts have been made to improve flight time of UAVs with electric propulsion. These include the incorporation of solar panel for mid-flight recharging, automatic recharging upon reaching destinations, but all require extra weights and additional electronic components that may cause magnetic interference.

Energy storage system's limitation restricts typical UAV flight time to not more than 30 minutes, and larger ESS adds more weight despite providing higher power capacity [31]. Hence, battery life has been a limiting factor for many applications [5]. Therefore, battery management and battery scheduling that optimise the State of Health (SoH) and reduce depth of discharge (DoD) and aging rate should be considered [31].

These include selecting an optimum battery capacity, monitoring its state of charge (SoC) and operating temperature, controlling the cycles of charging and timely charge and discharge constraints of the battery.

Despite limitations to the total flight time available, electrical propulsion still remains as the best options to power up UAVs today [6], in light of awareness of the harms of internal combustions including heat, emission and audible noises [32].

Capacity to mass ratio is a crucial consideration in selecting the ESS for a quadcopter. Li-Po battery is often used in this application because of its high energy density. Lithium batteries have the highest specific energy, while Li-Po battery is one of the safest types of lithium battery [26].

Table 1.3: Characteristics of different types of batteries

Battery type	Cell Voltage, V	Specific Energy (MJ/kg)
Lead acid	2.1	0.14
NiCd	1.2	0.14
NiMH	1.2	0.36
NiZn	1.6	0.36
Lithium (LiFePO4 or Li-Po)	3.3-3.7	0.4-0.7

Extra caution, however, is still required when using a Li-Po battery. The nominal voltage of individual Li-Po battery cell is 3.7V. Fully charged cell has a voltage of 4.2V. Discharging the cells below 3V is can cause permanent damage and inflammation. Therefore, monitoring the battery voltage during the multirotor autonomous flight is extremely important [19].

The C rate of a Li-Po battery measures the current per capacity of the battery [10].

$$C = \frac{I}{Ah} \quad (2.26)$$

For a Li-Po battery pack with 3 series cells the C rate

$$C = \frac{I_{cell}}{Ah} S \quad (2.27)$$

Where I_{cell} = Maximum current output per cell

This can be rewritten as

$$R_i = \frac{v.d. \times S}{Ah C} \quad (2.28)$$

Where:

R_i = Internal resistance of the battery (Ω)

v.d. = Voltage drop across the internal resistance of battery per cell (V)

Ah = Battery capacity of the battery (Ah)

C = C rating of the battery

S = Number of cells of battery

The maximum current draw from the battery is limited by the C rating of the battery

$$I_{max} = C \times Ah \quad (2.29)$$

From equation 2.29, during the discharge of battery, the capacity, Ah of the battery gradually reduces, and the maximum possible current that can be drawn from the battery will also decrease.

If equation 2.28 is modified with total resistance, R_{Total} across the connected circuit,

$$R_{total} = \frac{v.d. \times S}{Ah C} = \frac{VD}{Ah C} \quad (2.30)$$

Where

VD is the battery voltage

It is shown that reduced capacity, Ah after discharge also causes v.d., that is the voltage of the cell to drop. Voltage level must not be discharged to lower than 3 V per cell to avoid the capacity of the battery being too low for a recharge, or the current falls below the required motor drives' draw [33]. Note that the I_{max} value must always be more the sum of all current draw from all the rotors.

Enrouting a journey for better ESS, hybrid propulsion in UAVs has a balanced trade-offs between flight time and factors such as heat, emissions, noise, and efficiency, but incur higher initial investment costs [26]. Besides that, solar power is also widely used in combination with modified electric propulsion systems in high-performance UAVs [34].

2.3 System Architecture

Several researches probed into the use of Raspberry Pi for the movement and control of quadcopter from remote transmitter. A simple model presented is the fundamental of the drone's system architecture, which lays the foundation of this project. Detailed system architecture of this project is elaborated in Chapter 3.

Figure 1.14 lays the foundation of basic drone's system architecture. Command signals are sent wirelessly to the receiver which communicates with the Raspberry Pi. Additional features such as camera or navigation can also be added to the Raspberry Pi [21].

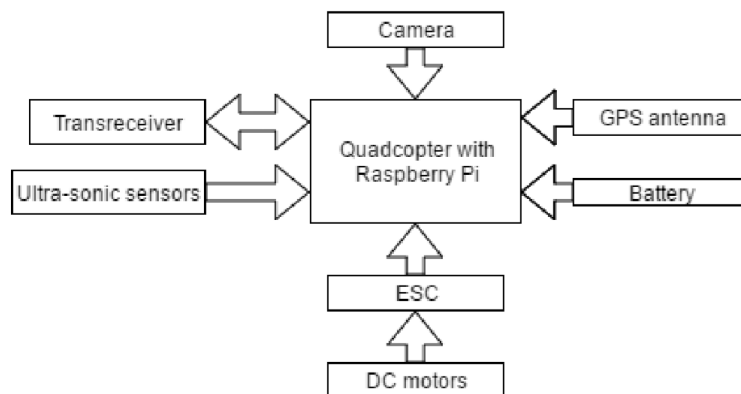


Figure 1.14: Simplified system architecture [21]

A method of improving the system architecture and control system of the quadcopter is through a sensor fusion technique, called Extended Kalman Filter (EKF), a new algorithm developed in the latest versions of FC using combined information from both the IMU and GPS for better accuracy [4].

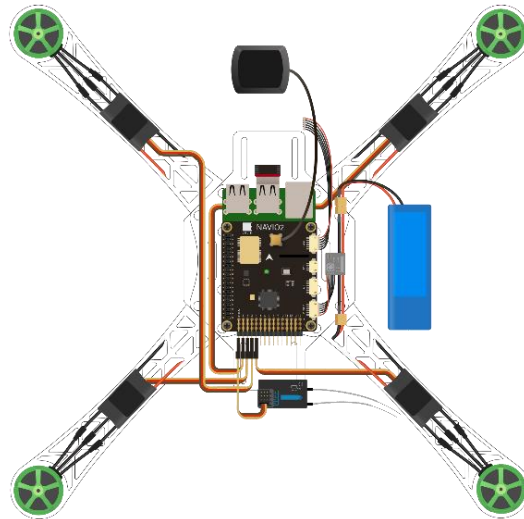


Figure 1.15: Quadcopter setup connection with navio2 [35]

A chassis is where all components and processors are mounted on. The chassis has to be strong to withstand loads and flexible so that it will not break apart easily. ESCs - mounted on the arms of the frame - control the rotor speed according to the transmitter's input or the sensors' feedback such as the accelerometer and gyroscope. The rotor turns the propellers whose blades generate thrusts [21]. Li-Po battery is used as the primary supply to the rotor as well as the FC when the quadcopter is in flight. The quadcopter's frame and propeller sizes, motor sizes and speeds, as well as the sizes of battery correlates with one another as in Table 1.4. The optimum size of battery with respect to the frame and propellers' size, motor sizes and speeds can be computed through ecalc.com, a platform for computations of various quadcopters' parameters.

Table 1.4: Quadcopter frame, battery, motor and propeller size matching [36]

<i>Frame Size/mm</i>	<i>Prop size/in</i>	<i>Motor size</i>	<i>Motor speed/KV</i>	<i>Li-Po size/mAh</i>
<i>120/smaller</i>	3	1104-1105	4000+	80-800 1S/2S
<i>150-160</i>	3-4	1306-1407	3000+	600-900 2S/3S
<i>180</i>	4	1806-2204	2600+	1000-1300 3S/4S
<i>210</i>	5	2204-2206	2300-2700	1000-1300 3S/4S
<i>250</i>	6	2204-2208	2000-2300	1300-1800 3S/4S
<i>330-350</i>	7-8	2208-2212	1500-1600	2200-3200 3S/4S
<i>450-500</i>	9-11	2212-2216	800-1000	3300+ 4S/5S